JOURNAL OF MATERIALS SCIENCE 17 (1982) 2979–2989

The fabrication and properties of Zr—O—F ceramics for the immobilization of Zircaloy nuclear waste

A. ATKINSON, A. K. NICKERSON, R. I. TAYLOR
Materials Development Division, AERE Harwell, Didcot, Oxfordshire, UK

The hot-pressing behaviour of hydrated zirconium oxide (with fluoride) derived from Zircaloy nuclear waste is described. The material densifies at relatively low temperatures to give a crystalline ceramic with monoclinic ZrO_2 and an oxyfluoride ($Zr_{10}O_{13}F_{14}$) as major phases. Doping with the inactive radwaste ions U^{4+}, Sr^{2+} and Cs^+ has shown that these should be taken into solid solution in the ceramic at the levels at which they are likely to be present in actual waste. Dissolution tests are described which establish that the ceramics are resistant to attack by water and hence should provide suitable leach-resistant hosts for the immobilization of the radwaste ions.

1. Introduction

Waste Zircaloy* fuel cladding is produced during the reprocessing of fuel from water-cooled nuclear reactors (e.g. PWR). Consequently there is interest in devising schemes to convert the Zircaloy into a more stable form suitable for long-term storage or eventual disposal. One possible stable form is as a ceramic of oxidized zirconium which is resistant to attack by water and it is with this option that the work described here is concerned.

The first step in any process leading to an eventual ceramic must be oxidation of the Zircaloy. A suitable method to achieve this is currently being developed at Harwell [1]. The basis of the method is to dissolve the Zircaloy in ammonium fluoride to give an ammonium fluozirconate ($(NH_4)_2ZrF_6$) solution from which the oxidized Zr is precipitated as a hydrated oxide (e.g. $ZrO_2 \cdot 2H_2O$) by the addition of ammonium hydroxide. The "hydrated zirconium oxide" is then the feed material for subsequent ceramic processing.

Radioactive isotopes are present in the waste Zircaloy from two sources. The Zircaloy itself is contaminated by activation products and isotopes which have been implanted into, or absorbed onto, its surface. The level of this activity is ~ 1000 Ci (β, γ) per tonne of Zircaloy (3.7×10^{13} Bq). In addition, fission products and unreacted fuel are present from incomplete separation of the fuel from the cladding. If the fuel contamination is 0.01% of that present before de-canning, this represents approximately a further 200 Ci (te Zircaloy)$^{-1}$ of β, γ activity (7.4×10^{12} Bq) and a further 20 Ci (te Zircaloy)$^{-1}$ of α-emitters (7.4×10^{11} Bq). The more significant of the radioisotopes are shown in Table I. It can be seen that the major radioisotopes in the short term are ^{137}Cs, ^{90}Sr and ^{125}Sb, and in the long term ^{239}Pu. The final column of Table I indicates that these isotopes are present at very low chemical concentrations (typically a few ppm by weight); U being the most abundant contaminant with a concentration of 0.15% by weight (U/Zr atom ratio = 6×10^{-4}).

The objective of the work described here was to define a hot-pressing route to convert the "hydrated zirconium oxide" precipitate into a high-density ceramic and to assess the suitability of the ceramic as a host for the immobilization of the entrained radioisotopes.

2. Characterization of "hydrated zirconium oxide"

The white voluminous precipitate from the ammonium fluozirconate solution was tray-dried

*Zircaloy-4 is an alloy of composition (in wt %) 98.2 Zr, 1.5 Sn, 0.2 Fe, 0.1 Cr.

0022–2461/82/102979–11$03.82/0

TABLE I Typical levels of signficant contaminants in 1 tonne waste Zircaloy containing 0.01% of its original fuel [1]

Isotope	Half-life (y)	Activity (Ci)	Mass (g)
^{60}Co	5.26	30	
^{90}Sr	28.1	30	0.4
^{125}Sb	2.7	400	1.6
^{134}Cs	2.05	150	2.6
^{137}Cs	30	500	70
^{239}Pu	2.44×10^4	20	4
U			1500

and then ball-milled to give a uniform powder. This material was inevitably contaminated with fluoride ions and this has important consequences for the final ceramic. Therefore, the fluorine content of the material is a significant variable. We have used two batches of "hydrated zirconium oxide" having different fluorine concentrations. One batch had a F/Zr atom ratio of 0.16 ± 0.02 and the other had $F/Zr = 0.47 \pm 0.04$. (The F/Zr ratios were measured by electron probe microanalysis (EPMA) of polished sections of the final ceramics.)

X-ray diffraction of the starting powder (Fig. 1a) revealed that it was mainly amorphous and this was confirmed by transmission electron microscopy (TEM) as illustrated in Fig. 2a. The crystalline diffraction peaks which are superimposed on the amorphous background in Fig. 1a could not be rigorously identified. Their pattern is similar to that of $KZrOF_3 \cdot 2H_2O$ and could well be characteristic of the ammonium analogue of this compound.

Thermogravimetric analysis (TGA, Fig. 3) revealed loss of volatile material at all temperatures; the integrated weight-loss being approximately 33% of the initial weight. Differential thermal analysis (DTA, Fig. 3) showed that the weight losses at both low and high temperatures were occurring endothermically. At low temperatures this corresponds to the volatilization of both water and probably NH_4F. This is confirmed by Fig. 1b which shows X-ray diffraction from material heated to 300° C. The lines corresponding to the ammonium fluozirconate are no longer present and the amorphous material has crystallized into monoclinic ZrO_2. Fig. 2b is a micrograph of the material at this stage. Most particles have a regular crystalline appearance and the small crystallite size (~ 10 nm) accounts for the broad

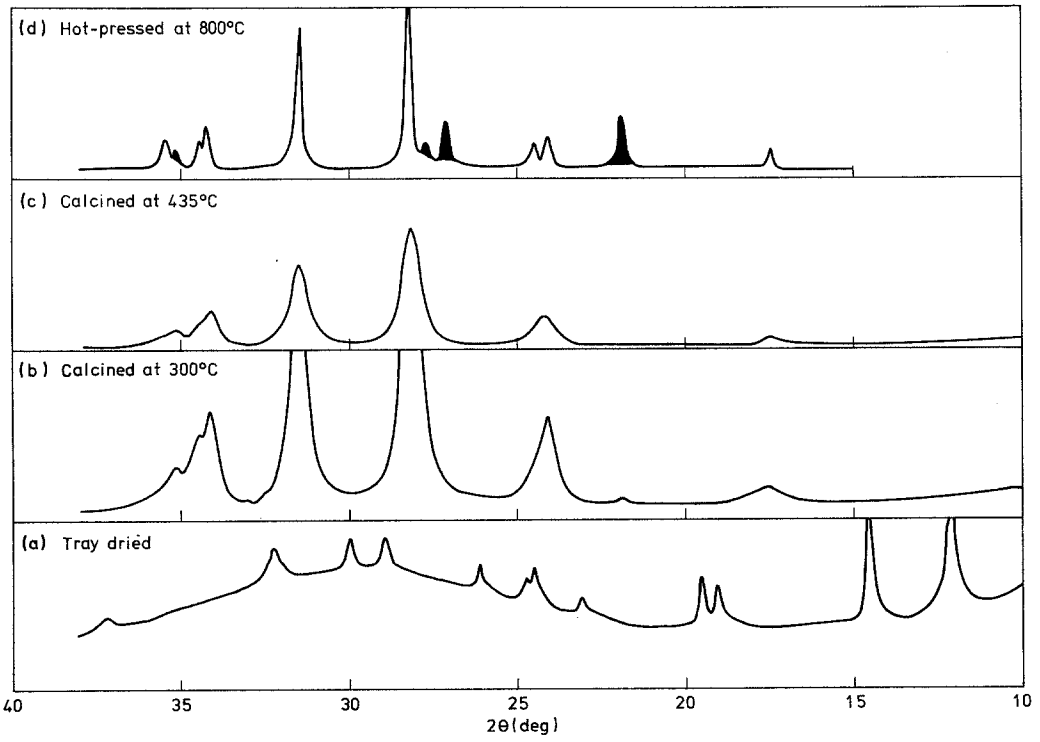

Figure 1 X-ray diffraction patterns (Cu$K\alpha$ radiation) from "hydrated zirconium oxide" (F/Zr = 0.47) after various heat treatments: (a) tray dried; (b) calcined for 2 h at 300° C (showing monoclinic ZrO_2); (c) calcined for 2 h at 435° C; (d) hot-pressed (30 min, 22.5 MPa) at 800° C (the shaded peaks are from zirconium oxyfluoride).

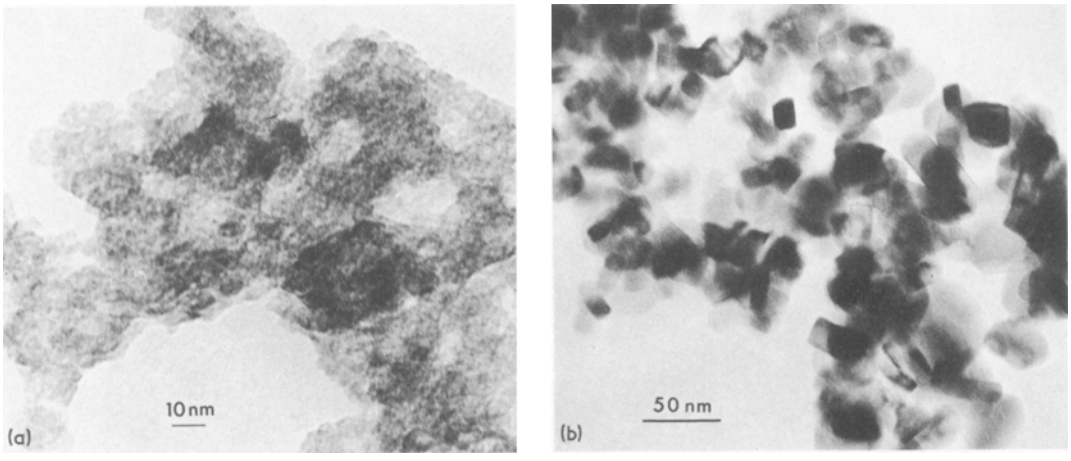

Figure 2 Transmission electron micrographs of "hydrated zirconium oxide" (F/Zr = 0.47); (a) tray dried; (b) calcined for 2 h at 300° C.

X-ray diffraction peaks. Although the stable bulk form of ZrO_2 at temperatures below 1100° C has the monoclinic structure, it is usually observed to have the tetragonal structure when the crystallite size is less than 30 nm [2]. It is thought that the presence of fluorine helps to stabilize the monoclinic form even when finely divided [3].

The weight-loss observed at high temperatures is probably caused by the volatilization of ZrF_4 which sublimes at 906° C (melting point 932° C) when pure. The DTA and TGA analyses (Fig. 3) also reveal an exothermic reaction occurring at 400° C which is accompanied by a loss in weight. X-ray diffraction of material heated to 435° C (Fig. 1c) shows no detectable structural change to have occurred.

3. Hot-pressing

Hot-pressing was carried out in cylindrical graphite dies of 12 mm internal diameter and at a pressure

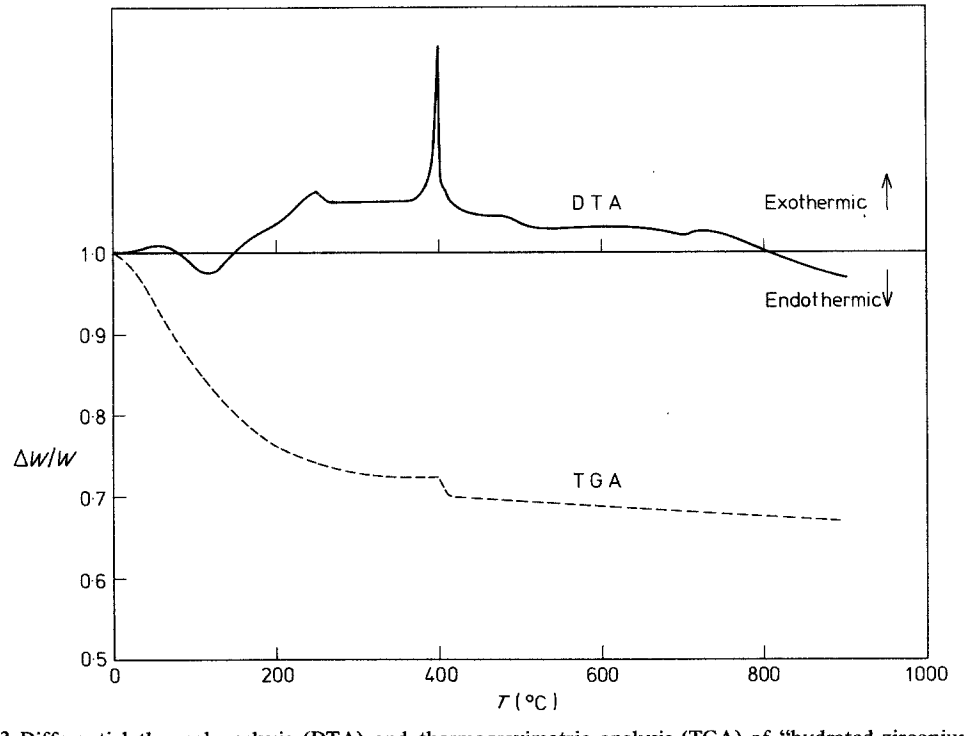

Figure 3 Differential thermal analysis (DTA) and thermogravimetric analysis (TGA) of "hydrated zirconium oxide" (F/Zr = 0.47). The heating rate was 10° C min^{-1}.

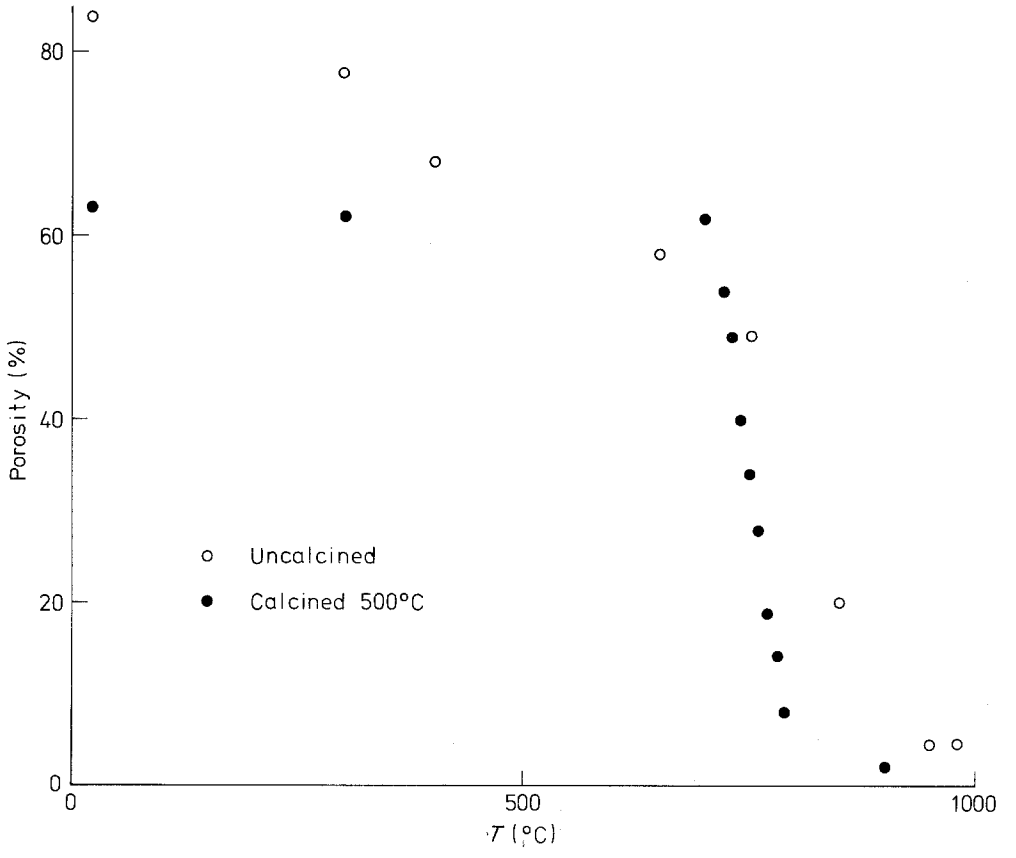

Figure 4 Elimination of porosity during hot-pressing at 22.5 MPa of "hydrated zirconium oxide" with F/Zr = 0.16 (note, heating rate 7.5° C min^{-1} up to 500° C for uncalcined material). The final porosity is estimated from the apparent density relative to the theoretical density.

of 22.5 MPa which was maintained constant throughout the temperature cycle. The heating-rate was 10° C min^{-1} and the final hot-pressed pellets were in the form of right cylinders.

Typical densification curves for both uncalcined and calcined material are shown in Fig. 4, from which it can be seen that for the calcined material densification begins suddenly at ~ 700° C. The final density as a function of top temperature during the hot-pressing cycle is shown in Fig. 5. The theoretical density was estimated from the phases known to be present in the final ceramic (see Section 4). The data demonstrate that ceramics can be fabricated with less than 2% residual porosity by hot-pressing at a top temperature $\geqslant$ 800° C. The final density of ceramics produced by hot-pressing at 980° C was found to be insensitive to the time (in the range 20 to 60 min) spent at the top temperature.

The hot-pressing behaviour was also found to be insensitive to the calcination temperature (calcination time 2 h) in the range 300 to 640° C i.e. the exothermic reaction which occurs at 400° C does not appear to be important. The uncalcined material could be successfully consolidated, albeit to a slightly lower density than the calcined material, provided that the heating rate was low enough to allow volatile material to escape from the die (Figs. 4 and 5). Calcining at too high a temperature, on the other hand, may result in a material which cannot be densified at temperatures below 1000° C, e.g. when calcined at 980° C (see Fig. 5).

The most likely reason for the difficulty in densifying material which has been calcined at too high a temperature is that as the calcination temperature is increased, more fluorine is lost by evaporation of ZrF_4. When uncalcined material with F/Zr = 0.16 initially was calcined at 640° C the fluorine content was reduced to F/Zr = 0.04 ± 0.01 and when calcined at 980° C to F/Zr = 0.005 ± 0.002 (measured in the final ceramics). That the presence of F is necessary for densification below 1000° C was demonstrated

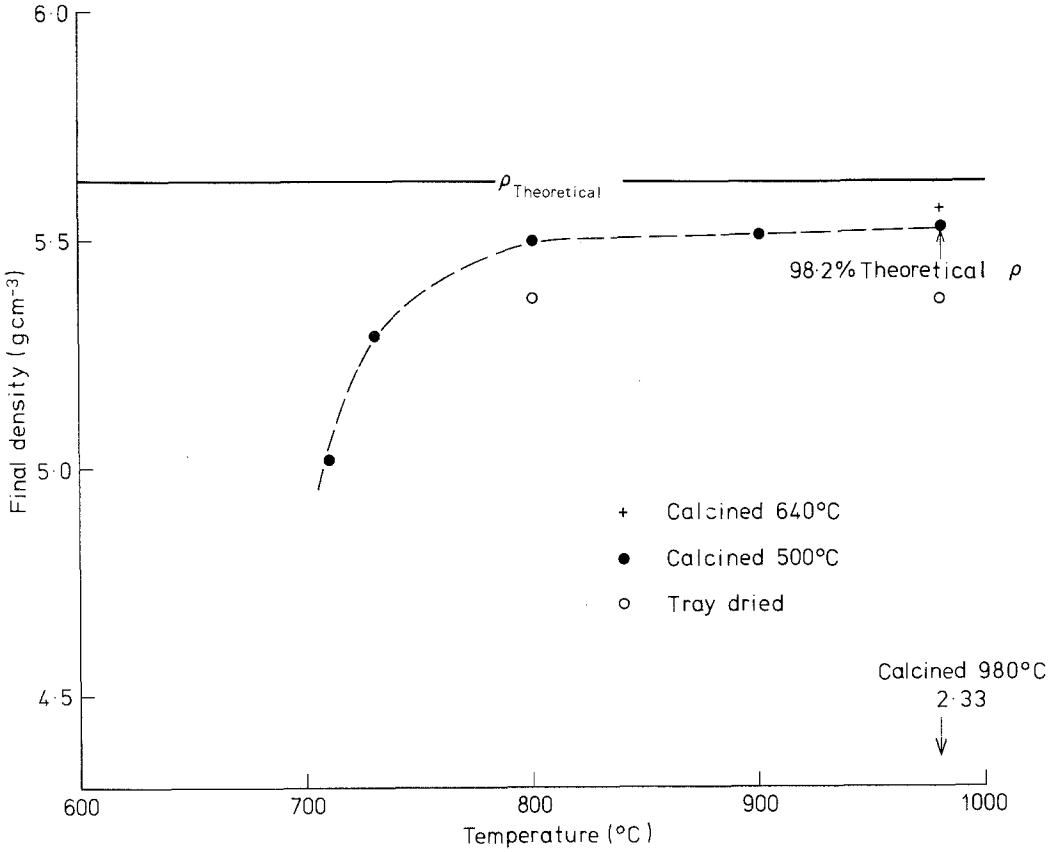

Figure 5 Final density as a function of top temperature after a hot-pressing cycle with a hold of 30 min at the top temperature (F/Zr = 0.16).

by hot-pressing zirconia powders produced by a sol–gel route [4]; one without F and the other with F/Zr = 0.1. The final densities after calcining at 450° C and hot-pressing at 980° C were 3.6 and 5.4 g cm^{-3}, respectively. Therefore, it is concluded that F above a critical concentration is required for low-temperature densification and that this critical value is in the range $0.005 < (F/Zr)_{crit} < 0.04$.

4. Microstructure

X-ray diffraction (XRD) of the hot-pressed ceramics revealed that they were mixtures of monoclinic ZrO_2 and at least one zirconium oxyfluoride compound (e.g. Fig. 1d). The crystallography of phases in the ZrO_2–ZrF_4 system has been studied by Holmberg [5] and by Joubert and Gaudreau [6]. The oxyfluorides which form within this system are classified according to whether their parent structures are of the CaF_2, α-U_3O_8 or ReO_3 types. These structures have anion to cation ratios corresponding to the formulae MX_2, $MX_{2.667}$ and MX_3, respectively. Since the addition of ZrF_4 to ZrO_2 increases the anion to cation ratio, then as the F/Zr ratio is increased one progresses through the sequence of structure types mentioned above. The oxyfluorides based on the orthorhombic α-U_3O_8 structure (which is, in turn, based on hexagonal α-UO_3) are particularly important in the case of the ceramics being described here. They are believed to form a sequence of compounds having the general formula [7] $M_{3n-4}X_{8n-10}$ ($n = 4, 6, 8, \ldots$), i.e. $Zr_{3n-4}O_{4n-6}F_{4n-4}$. The end members of this sequence are $Zr_4O_5F_6$ (i.e. $MX_{2.75}$) and $Zr_3O_4F_4$ (i.e. $MX_{2.667}$). In addition, F is known to dissolve in ZrO_2 to form an ordered solid solution of composition $ZrO_{1.917}F_{0.167}$ [6] and has a structure very similar to that of monoclinic ZrO_2 (i.e. based on the CaF_2 parent structure).

Detailed comparison of X-ray diffraction data from the hot-pressed ceramics with previously published data revealed that all the diffraction data could be explained by the presence of only two phases in the ceramics. These are monoclinic ZrO_2 and the oxyfluoride $Zr_{10}O_{13}F_{14}$ ($n = 8$ in

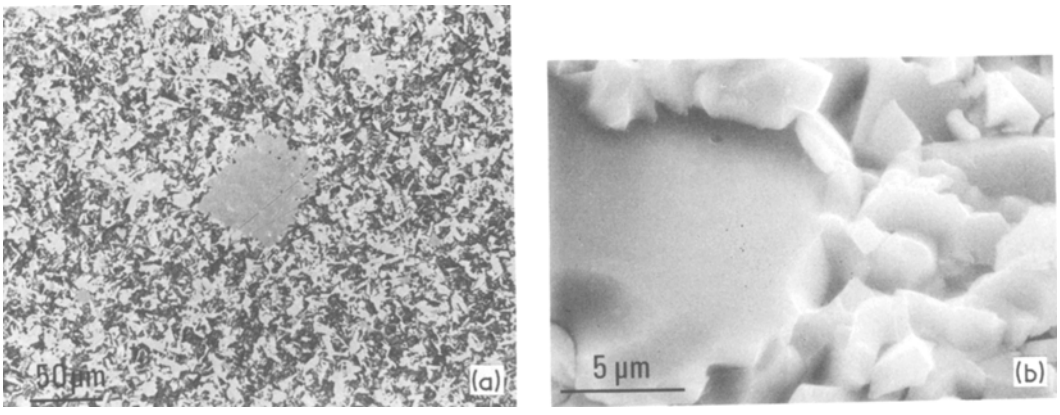

Figure 6 Microstructure of a hot-pressed Zr–O–F ceramic (F/Zr = 0.16, 30 min at 980° C, 22.5 MPa, $\rho = 5.53$ g cm^{-3}): (a) optical micrograph of a polished section; (b) scanning electron micrograph of a fracture face.

the general formula i.e. $MX_{2.70}$). The relative amounts of the two phases depend on the F/Zr ratio of the material. The theoretical density referred to in Section 3 was calculated from the F/Zr ratio (f) and the theoretical densities of the two pure phases; 5.826 g cm^{-3} for ZrO_2 and 4.57 g cm^{-3} for $Zr_{10}O_{13}F_{14}$. The expression for the density is

$$\rho = 5.826 \frac{(1 + 0.089f)}{(1 + 0.311f)} \text{ g cm}^{-3}.$$

Fig. 6a is an optical micrograph of a polished section of a typical hot-pressed ceramic. The material was very difficult to polish owing to pluck-out of grains which accounts for the "mottled" appearance of the microstructure. However, two distinct phases can be seen, the darker phase showing a tendency to aggregate as illustrated in the centre of the field in Fig. 6a. Fluorine imaging by EPMA established that this darker phase is the oxyfluoride. The fracture surface of Fig. 6b shows small grains of the order of a few microns in size (and presumably ZrO_2) adjacent to one of the large particles (presumably oxyfluoride).

Thin foils prepared from the hot-pressed ceramics were examined by TEM and a typical example is shown in Fig. 7. Very little porosity can be seen and few dislocations were detected. Monoclinic ZrO_2 grains could be easily identified from their pseudo-cubic diffraction patterns. Some crystals with the basic monoclinic ZrO_2 structure generated lattice fringe images of ~ 3 nm spacing (Fig. 8a). The orthorhombic oxyfluoride could be most readily identified in the pseudo-hexagonal orientation and generated lattice fringe images of either ~ 3.9 nm spacing (Fig. 8b), or ~ 3.3 nm spacing (Fig. 8c).

5. Solid solubility of radwaste ions

The solid solution of the radwaste ions Cs, Sr and U in the zirconia and oxyfluoride phases of the ceramics was investigated by doping the "hydrated zirconium oxide" precursor with the appropriate dopant so that the atomic ratio of dopant to zirconium was approximately 0.03. Samples taken from close to the centre of the hot-pressed cer-

Figure 7 Transmission electron micrograph showing the microstructure of a hot-pressed Zr–O–F ceramic (F/Zr = 0.16, 30 min at 800° C, 22.5 MPa, $\rho = 5.50$ g cm^{-3}).

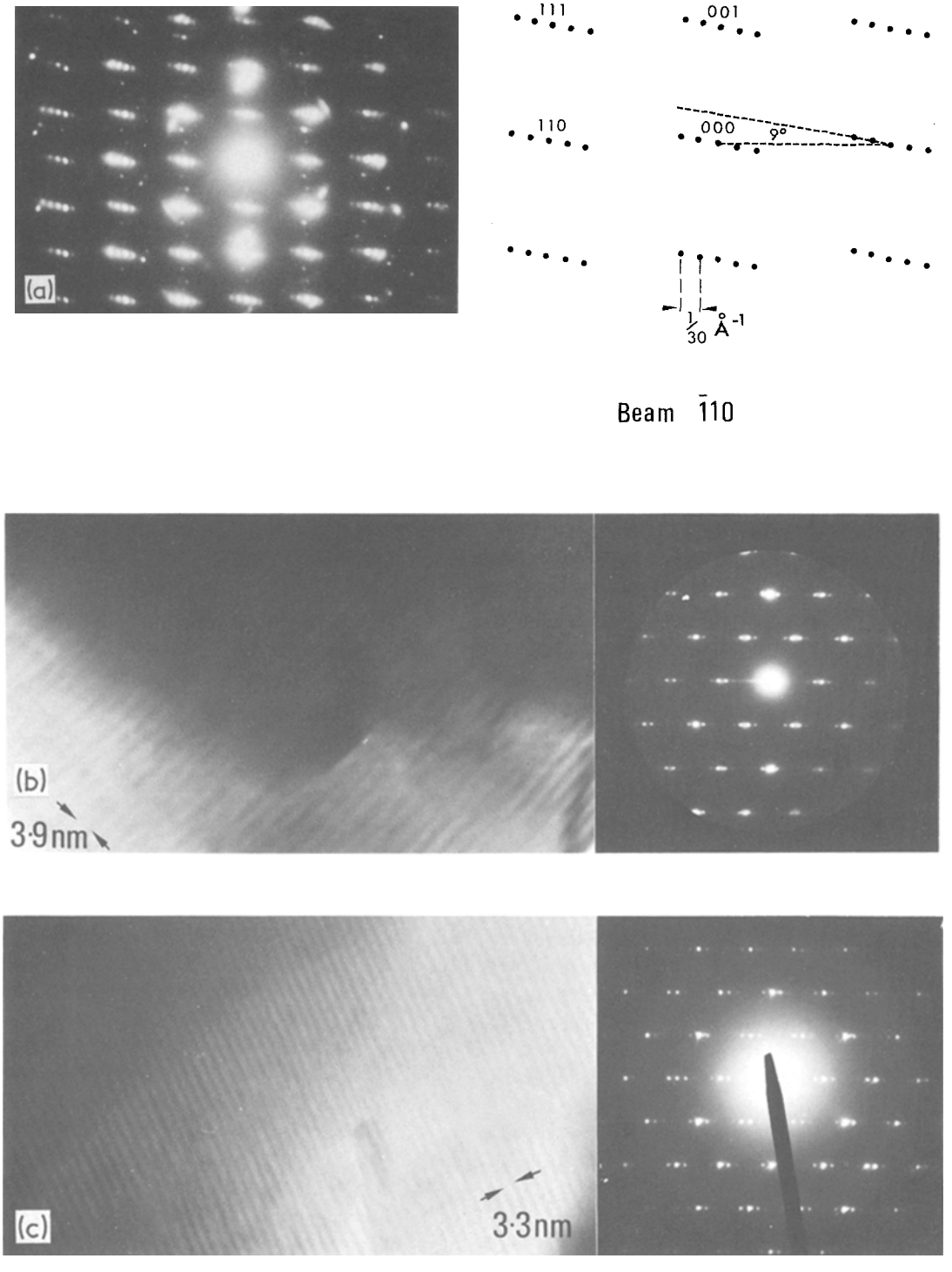

Figure 8 Transmission electron microscopy of "superlattice phases" in the hot-pressed ceramics. (a) Electron diffraction pattern of a superlattice phase with the monoclinic ZrO_2 basic structure. The main diffraction peaks are indexed according to the monoclinic reciprocal lattice. The superlattice spots are along the [1 0 0] direction of the reciprocal lattice and are seen along the projection of the [1 0 0] direction on to the ($\bar{1}$ 1 0) section. (b) Electron diffraction pattern and lattice fringe image of superlattice phase of spacing 3.9 nm based on hexagonal α-UO_3 (i.e. $Zr_{10}O_{13}F_{14}$). (c) Electron diffraction pattern and lattice fringe image of superlattice phase of spacing 3.3 nm based on α-UO_3 (i.e. $Zr_{17}O_{22}F_{24}$).

amics were crushed and the powder dispersed in isopropanol. Carbon-coated copper TEM grids were dipped into the dispersion and the material collected on the dried grids was examined in a Philips EM400 microscope equipped with facilities for the energy dispersive analysis of X-rays (EDAX). Individual crystallites were identified as being either monoclinic ZrO_2 or oxyfluoride from their electron diffraction patterns and their composition (in terms of concentration of dopant ion) was determined by EDAX. All the materials inevitably contained some Sn from the Zircaloy. This was detected in the EDAX spectra at about equal concentrations in both the zirconia and oxyfluoride phases.

It should be emphasized that the doping level in these experiments is many orders of magnitude greater than the expected concentration of most radwaste ions in the actual waste material (see Table I).

5.1. Caesium doping

The Cs was introduced by dispersing tray-dried "hydrated zirconium oxide" (F/Zr = 0.47) in water containing dissolved CsF. Excess water was allowed to evaporate and then the material was calcined at 300° C and hot-pressed for 30 min at 980° C. (In one experiment some material was observed to condense on the water-cooled part of the hot-press close to the graphite die. This was identified by XRD as a mixture of monoclinic ZrO_2 and Cs_2ZrF_6 and was presumably formed by volatilization of the caesium fluozirconate during hot-pressing). XRD of the hot-pressed ceramics revealed a diffraction peak corresponding to an interplanar spacing of 0.352 nm which could not be ascribed to the Zr–O–F system, nor any likely compound to Cs.

When the crushed ceramics were examined by TEM no Cs could be detected in any crystals of monoclinic ZrO_2 which were analysed. This not only demonstrates that the solubility of Cs in ZrO_2 is below the limits of detection (i.e. $Cs/Zr < 10^{-3}$) but that the analysis is not being perturbed by any Cs contamination of the surfaces of the crystallites. On the other hand, Cs could be detected in some crystals of oxyfluoride; a Cs/Zr atom ratio of 4×10^{-3} being typical. Occasionally crystals whose diffraction patterns could not be identified were found which contained much larger Cs concentrations, up to $Cs/Zr \simeq 0.5$.

5.2. Strontium doping

The Sr was added to the "hydrated zirconium oxide" (F/Zr = 0.47) in the same way as described for Cs except that strontium nitrate was used in aqueous solution because of the low solubility of strontium fluoride. The calcined material was hot-pressed for 30 min at 800° C.

XRD of the hot-pressed ceramics showed only zirconia and oxyfluoride, but with extra diffraction peaks at 0.382 and 0.308 nm which could not be attributed to any known likely Sr-containing compounds. In TEM, Sr could be detected in monoclinic zirconia crystals at various concentrations whereas it was only just detectable ($\sim 2 \times 10^{-3}$ atom fraction) in the oxyfluoride. One crystal of monoclinic ZrO_2 was found with a Sr/Zr ratio of approximately unity.

5.3. Uranium doping

In this case uranium fluoride was added to the ammonium fluozirconate solution prior to precipitation of the "hydrated zirconium oxide". The tray-dried product had $F/Zr \simeq 1.5$ which was high enough to produce some $ZrO_{0.45}F_{3.1}$ in the hot-pressed ceramic. The doped precipiate was therefore "diluted" with commercial ZrO_2 (> 99.8% purity) by ball-milling to reduce F/Zr to ~ 0.7. After calcination the material was hot-pressed for 30 min at 800° C. Uranium was found in solid solution in both the ZrO_2 and the oxyfluoride phases.

6. Properties of the hot-pressed ceramics

6.1. Dissolution in water

The resistance of the ceramics to attack by water has been assessed by using both Soxhlet and MCCI* standard dissolution tests. The Soxhlet test is a reflux test at ~ 100° C and the dissolution rate was determined from the weight change of the specimen before and after the test. The MCCI test is a series of experiments on different specimens each in an equal fixed volume of static liquid. The dissolution data in this case were obtained both from weight changes and from chemical analysis of the leachate solutions (i.e. the liquid on terminating the test). The specimens were tested with surfaces in the as-machined condition and ultrasonically cleaned in acetone before testing.

The specimens tested by the Soxhlet method were discs 12 mm diameter x 2 mm thickness and

*As specified by the Materials Characterisation Center, Battelle Pacific Northwest Laboratories, Richland, USA.

TABLE II Dissolution of Zr–O–F ceramics measured by Soxhlet test for 3 days at 100° C

F/Zr atom ratio	Pressing temperature (° C)	Density (g cm^{-3})	Percentage weight change	Dissolution rate (g cm^{-2} day^{-1})
0.16	980	5.53	−0.13	1.6×10^{-4}
0.16	980	5.38	−0.27	3.2×10^{-4}
0.16	800	5.50	+0.12	
0.16	730	5.29	+0.27	
0.16	710	5.02	+0.32	
0	Single crystal	5.83	−0.067	2.5×10^{-5}
1.43 ($Zr_7O_9F_{10}$)	980	4.58	−0.015	1.4×10^{-5}

the duration of the test was 3 days. The average rates of dissolution (based on the weight change and the geometric external surface area) are shown in Table II. The shortcomings of the Soxhlet testing method are immediately obvious from the table since some specimens actually increased in weight during the test presumably as a result of a hydration reaction. Nevertheless the results demonstrate the low dissolution rates of these ceramics and in particular indicate that the oxyfluoride phase is not readily soluble.

The MCCI static test was carried out using high-purity water at 90° C and a volume of 17 ml per specimen. The specimens were rectangular blocks 7 mm × 5 mm × 4 mm and were all cut from the same billet which had been hot-pressed for 30 min at 800° C. The mean density of the material was 95% theoretical density and the F/Zr ratio 0.47. The Zr concentration in the leachate solution was measured by atomic emission in an inductively coupled discharge and the F concentration by ion-chromatography. The results are presented in Fig. 9 together with the weight-change data and the pH of the leachate measured at room temperature after testing. The error bars were estimated by using two different specimens for each test time. The data in Fig. 9 show that the dissolution rate is not constant. However, from the dashed lines (which correspond to a constant dissolution rate of 10^{-4} g cm^{-2} d^{-1} or 1.16×10^{-8} kg m^{-2} sec^{-1}) it is evident that the extent of dissolution is broadly consistent with the results of the Soxhlet tests. Fig. 9 also shows that although the concentrations of F and Zr have reached constant values for times beyond 5 days, the weight change measurements indicate that a reaction is still taking place which does not involve the transfer of Zr or F into solution. The F/Zr atom ratio in the leachate solution is 4.1 which establishes that ZrF_4 is being leached from the ceramic.

6.2. Mechanical strength

The rupture stress of the ceramic was measured using centrally loaded machined discs 12 mm diameter × 1.5 mm thickness. The mean value of the rupture stress for material with F/Zr = 0.16 hot-pressed for 30 min at 980° C was 150 MPa.

7. Discussion

The presence of F, even at low concentrations, is a very effective densification aid for hot-pressing ZrO_2 at relatively low temperatures. Stuart *et al.* [8] have reported that F is an effective densification aid for ThO_2 (which is very similar to ZrO_2 in its structure and properties). They attributed the beneficial effect of F on densification as resulting from "microsintering" which is facilitated in its presence. This they support by presenting evidence to show that the exothermic DTA peak which they observe only in the presence of F (c.f. that in Fig. 3) is accompanied by growth in crystallite size and reduction in specific surface area. However, this behaviour was not observed here in the case of the "hydrated zirconium oxide" since XRD indicated no significant growth in crystallite size (Fig. 1) at the temperature of the exothermic reaction (400° C). Furthermore, this temperature is much lower than that at which rapid densification begins (~ 700° C). Therefore it appears that "microsintering" is not the reason for the beneficial effect of F. Rather, the segregation of oxyfluoride into relatively large volumes (e.g. Fig. 6a) suggests that there may have been a F-containing liquid forming at ~ 700° C during hot-pressing which has assisted densification.

To test this hypothesis a specimen of oxyfluoride having F/Zr = 1.4 was prepared by hot-pressing. However, DTA of this material showed no evidence of melting at temperatures up to 1000° C. It may be that the liquid is formed only under external pressure because the calcined

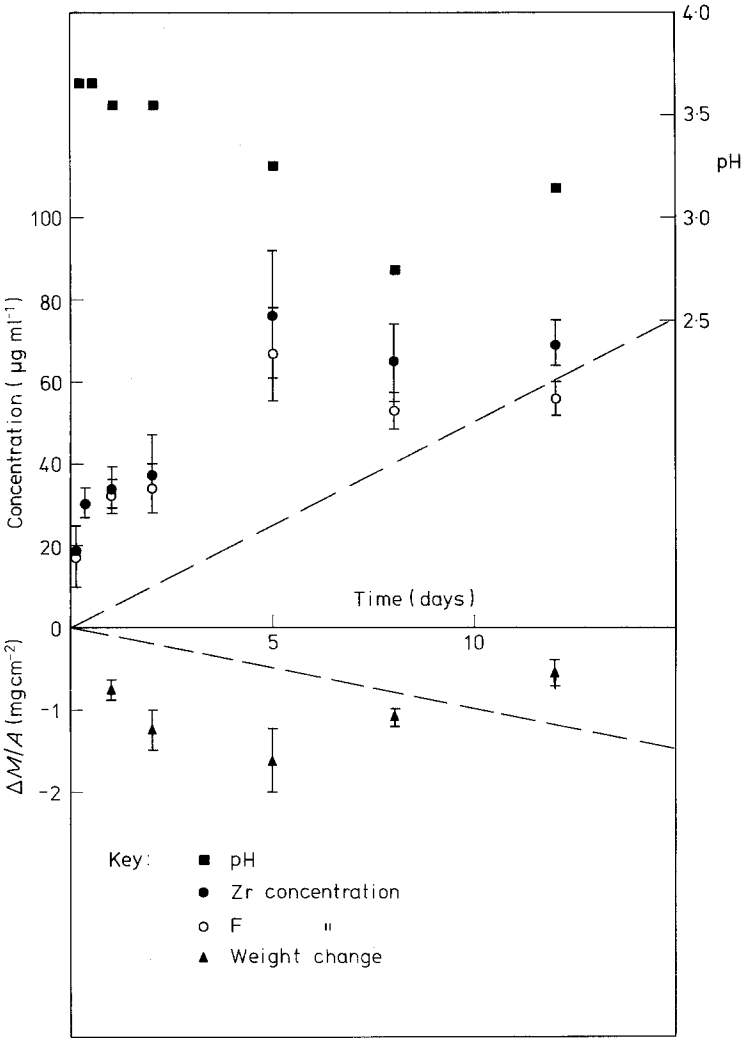

Figure 9 Dissolution test at 90° C (MCCI specification) on Zr–O–F ceramic (F/Zr = 0.47) hot-pressed at 800° C (96% theoretical density). The upper part of the figure shows the concentration of species in the liquid whereas the lower part shows the change in weight of the solid. The dashed lines represent a dissolution rate of 10^{-4} g cm^{-2} d^{-1}.

"hydrated zirconium oxide" could not be densified by cold-pressing followed by sintering at temperatures up to 1000° C. Therefore the mechanism of densification during hot-pressing remains obscure.

According to Joubert and Gaudreau [6] the equilibrium phases in the hot-pressed ceramics should have been $ZrO_{1.917}F_{0.167}$ for material with F/Zr = 0.16 and a mixture of this phase and $Zr_{10}O_{13}F_{14}$ for F/Zr = 0.47. However, in the actual hot-pressed ceramics the two main phases, for both F/Zr ratios, were monoclinic zirconia and $Zr_{10}O_{13}F_{14}$. Such oxyfluorides of general composition $M_{3n-4}X_{8n-10}$ (see Section 4) are orthorhombic with one of the unit cell dimensions being $(3n-4)/2$ times the unit cell dimension of the hexagonal α-UO_3 parent structure (0.389 nm) [7]. Thus crystals of $Zr_{10}O_{13}F_{14}$ have $n = 8$ and should generate superlattice diffraction spots in TEM corresponding to a spacing of 3.9 nm (e.g. Fig. 8b). The compound $Zr_7O_9F_{10}$ has $n = 6$ and therefore has a superlattice spacing of 2.7 nm. This superlattice spacing was not observed in any crystals from the hot-pressed ceramics, but crystals having a spacing of 3.3 nm were observed (Fig. 8c). This superlattice can result from an intergrowth of the two ideal superlattices to give a crystal of intermediate composition ($Zr_{17}O_{22}F_{24}$) as described by Papiernik *et al.* [7] for the ZrO_2–UF_4 system. The crystals with the basic monoclinic ZrO_2 structure which showed superlattice spacings of 3 nm (Fig. 8a) were probably of composition $ZrO_{1.197}F_{0.167}$ (i.e. $Zr_{12}O_{23}F_2$). Crystals of this compound have, in fact, an orthorhombic superlattice with superlattice planes of 3 nm spacing parallel to either the (1 0 0) or (0 0 1) planes of

the basic monoclinic structure. The electron diffraction pattern of Fig. 8a can be interpreted satisfactorily in these terms. Thus it is apparent that the hot-pressed ceramics have not reached equilibrium during hot-pressing since they are composed of different phases sfrom those expected from the known equilibria. (These minority phases were not detected by XRD because their structures are so similar to the respective majority phases).

The observation that both ZrO_2 and the oxyfluorides can take U^{4+} into solid solution was to be expected from the studies of Gaudreau and coworkers [6, 7] and the general similarity between U^{4+} and Zr^{4+} ions (of radii 0.1 and 0.084 nm, respectively, in eight-fold co-ordination). Therefore these ceramics should be particularly good hosts for U, Pu and other radwaste actinides. The radius of the Sr^{2+} ion in eight-fold co-ordination is somewhat larger (0.125 nm) but, nevertheless, is believed to have limited solid solubility [9] ($Sr/Zr \simeq 5 \times 10^{-2}$) in tetragonal ZrO_2 at high temperatures ($> 1600^\circ$ C). Some solid solubility of Sr in ZrO_2 is also expected from the known behaviour of the other group IIA ions Mg^{2+} and Ca^{2+} which dissolve readily in cubic ZrO_2 [2]. Thus the wide range of Sr/Zr ratios found in monoclinic ZrO_2 crystals in the hot-pressed ceramics probably reflects the non-equilibrium nature of the ceramics rather than extensive thermodynamic solid solution. The Cs^+ ion is very large (0.18 nm in eight-fold co-ordination) and is therefore unlikely to make a simple substitution into either ZrO_2 or the oxyfluoride because of purely geometrical constraints. The reason why the oxyfluoride was found to accept some Cs in solid solution may be because of its less dense, more disordered structure.

8. Conclusions

(1) "Hydrated zirconium dioxide" from the dissolution of waste Zircaloy can be hot-pressed at temperatures between 800 and 1000° C at a pressure of 22.5 MPa to give a high-density ceramic. The conditions for calcination prior to hot-pressing are not critical and can be chosen to suit the extent of removal of volatile material which is required. A calcination temperature of 500° C is the optimum in this respect.

(2) The presence of F in the "hydrated zirconium oxide" is necessary for densification at these low temperatures. The minimum critical F/Zr atom ratio required is somewhere in the range 0.005 to 0.04.

(3) The hot-pressed ceramics are composed of two principal phases; the relative amounts depending on total F concentration. The phases are monoclinic ZrO_2 (baddeleyite) and an orthorhombic oxyfluoride $Zr_{10}O_{13}F_{14}$ which has a defective α-UO_3 structure. ZrO_2 containing ordered substitutional F and an oxyfluoride with composition intermediate between $Zr_{10}O_{13}F_{14}$ and $Zr_7O_9F_{10}$, occur as minority phases.

(4) Both the monoclinic ZrO_2 and oxyfluorides were found to accept U^{4+} and Sr^{2+} ions in solid solution. Some Cs^+ was found in solid solution in the oxyfluoride.

(5) Both the monoclinic ZrO_2 and oxyfluoride phases have low dissolution rates in water. The oxyfluoride is preferentially attacked and ZrF_4 is released, but the resulting enrichment of ZrO_2 at the solid surface probably provides a protective layer which prevents further attack.

Acknowledgements

We wish to thank Dr H. A. Kearsey and Mr A. Mercer for providing the "hydrated zirconium oxide", Dr C. Pickford, Mr J. Gallaher and Mr F. Cullen for assistance with chemical and X-ray analysis, and Mr T. M. Valentine for Soxhlet dissolution tests. We also thank Mr J. S. Pottinger for his helpful advice. We are grateful to the Commission of the European Community and the Department of the Environment for financial support. In respect of the UK DoE interest, the results will be used in the formulation of Government policy but at this stage they do not necessarily represent Government policy.

References

1. A. C. MERCER and H. A. KEARSEY, private communication.
2. R. C. GARVIE, in "High Temperature Oxides, Part II", edited by A. M. Alper (Academic Press, New York, 1970) pp. 117–66.
3. S. A. SELIM and S. HANAFI, *Surface Technology* **12** (1981) 287.
4. J. L. WOODHEAD, *Sci. Ceram.* **4** (1968) 105.
5. B. HOLMBERG, *Acta Cryst.* **B26** (1970) 830.
6. P. JOUBERT and B. GAUDREAU, *Rev. Chim. minérale* **12** (1975) 289.
7. R. PAPIERNIK, B. GAUDREAU and B. FRIT, *J. Sol. State Chem.* **25** (1978) 143.
8. W. I. STUART, T. L. WHATELY and R. B. ADAMS, *J. Australian Ceram. Soc.* 8 (1972) 6.
9. T. NOGUCHI, T. OKUKO and O. YONEMOCHI, *J. Amer. Ceram. Soc.* **52** (1969) 181.

Received 1 March
and accepted 22 March 1982